Postprint version of paper published in Computers & Chemical Engineering, 2014, Volume 61 Pages38–50.
The content is identical to the published paper, but without the final typesetting by the publisher.

Tuning of NMPC controllers via multi-objective optimisation

Mattia Vallerio[a], Jan Van Impe[a,*], Filip Logist[a]

[a] *BioTeC & OPTEC, KU Leuven, Department of Chemical Engineering, W. de Croylaan 46, B-3001 Leuven, Belgium*

Abstract

Nonlinear Model Predictive Control (NMPC) is a powerful technique that can be used to control many industrial processes. Different and often conflicting control objectives, e.g., reference tracking, disturbance rejection and minimum control effort, are typically present. Most often these objectives are translated into a single weighted sum (WS) objective function. This approach is widespread because it is easy to use and understand. However, selecting an appropriate set of weights for the objective function is often non-trivial and is mainly done by trial and error. The current study proposes a systematic procedure for tuning Nonlinear MPC based on multi-objective optimisation methods. Advanced methods allow an efficient solution of the multi-objective problem providing a systematic overview of the controller behaviour. Moreover, through analytic relations it is possible to link a solution obtained with these novel methods to a set of weights for a weighted sum objective function. Applying this set of weights causes the WS to generate the same solution as obtained with the advanced method. Hence, an appropriate controller can be selected based on the alternatives generated by the advanced method, while the corresponding weights for a WS can be derived for implementing the controller in practice. The procedure is successfully tested on two benchmark applications: the Van de Vusse reactor and the Tennessee Eastman plant.

*Corresponding author

Email addresses: mattia.vallerio@cit.kuleuven.be (Mattia Vallerio), jan.vanimpe@cit.kuleuven.be (Jan Van Impe), filip.logist@cit.kuleuven.be (Filip Logist)

URL: http://cit.kuleuven.be/biotec/index.php (Filip Logist)

Postprint of manuscript accepted for Computers & Chemical Engineering

Journal homepage: http://www.journals.elsevier.com/computers-and-chemical-engineering/
Original file available at: http://dx.doi.org/10.1016/j.compchemeng.2013.10.003

Keywords: Multi-objective optimisation, Nonlinear Model Predictive Control, Nonlinear optimisation, Tennessee Eastman, Dynamic optimisation, ACADO toolkit

1. Introduction

Model Predictive Control (MPC) has been extensively studied and successfully applied to a number of real-life industrial problems (see for an overview [1, 2] and all the references therein). Several aspects contribute to the success of MPC: (i) its systematic approach to handle complex control problems with multiple inputs and outputs, (ii) its ability to explicitly incorporate constraints on state and control variables, (iii) its versatility enabling the control of a wide variety of applications in chemical, mechanical and electrical engineering, and (iv) its optimisation based nature enabling an optimised process behaviour. Classic MPC involves a linear process model, linear constraints and a quadratic objective. During the last two decades extensions to Nonlinear MPC (NMPC) have been elaborated by allowing nonlinear process models, constraints and objective functions (see, e.g., [3, 4, 5, 6, 7]).

As (N)MPC is an optimisation based control strategy, an objective function has to be specified. Often this objective function is a weighted sum of different terms (e.g., deviations from selected setpoints). However, the selection of an appropriate set of weights, i.e., the tuning of the controller, is in general not a trivial task. Selecting different sets of weights allows trading off the different terms and generates different but mathematically equivalent solutions. In multi-objective optimisation, which aims at finding optimal solutions to multiple and conflicting objectives, these points are called Pareto optimal solutions [8]. From these Pareto optimal solutions, one has to be selected by the Decision Maker (DM) (e.g., the control engineer) according to his/her preferences and the selected set of weights has to be implemented in the controller.

Lately, the multi-objective nature of MPC tuning has been explicitly recognised. An overview on the tuning of linear MPC controllers was written by [9, J. L. Garriga and M. Soroush]. For linear MPC [10, W. Wojsznis et al] prioritised the objectives by imposing increasing weights with the order of importance given to the objectives. [11, J.H. van der Lee et al.] presented

Postprint version of paper published in Computers & Chemical Engineering, 2014, Volume 61 Pages38–50.
The content is identical to the published paper, but without the final typesetting by the publisher.

a procedure for tuning of MPC controllers based on a multi-objective approach that exploits a genetic algorithm and fuzzy logic. [12, Bemporad and Muñoz de la Peña] proposed a novel algorithm based on the generation of the Pareto frontier and at each sampling time a selection of the desired control action is performed by the DM. In particular, the work focuses on the trade-off between closed-loop promptness and noise rejection. In addition, some criteria on how to select Pareto points in order to guarantee stability of the controller are given for the linear case.

On the NMPC side, two recent articles [13, V. M. Zavala] and [14, A. Flores-Tlacuachuac] opened new perspectives towards multi-objective model predictive control. In particular the proposed algorithm, does not require the expensive computation of the Pareto front but translates the problem into the tracking of the so called *utopia point* (i.e., the infeasible point that has as coordinates the optimal solution of all objectives taken one by one). In this implementation the decision maker does not have to make a choice at any step. It is assumed that the best solution is the one known as the *compromised solution*, i.e., the closest point to the *utopia point* but still belonging to the Pareto front. This approach exhibits several advantages from the on-line application point of view: (i) the Pareto front does not need to be generated at each NMPC step, (ii) it does not need weights to be adjusted or any other decision to be made. However, the selected point is determined by the shape and scaling of the Pareto set and may not always reflect the preferences of a DM.

The aim of the current work is to allow the decision maker to select an appropriate weight matrix for NMPC controllers in view of, e.g., grade transitions. A systematic presentation of possible optimal alternatives (i.e., the Pareto set) typically facilitates the selection by the decision maker. However, varying the weights of the weighted sum approach to approximate the Pareto set is conceptually easy but will in practice suffer from intrinsic drawbacks [15]. For instance, a systematic variation of weights does not necessarily lead to a uniform spread of solutions on the Pareto front. This explains the difficulties experienced by the practitioner to tune the weight matrix with a trial and error procedure. Reducing a weight and increasing another other does not necessarily lead to a proportional response in the results. The current work uses novel multi-objective approaches to generate an accurate representation of the Pareto set (e.g., Normal Boundary Inersection (NBI) [16],

Journal homepage: http://www.journals.elsevier.com/computers-and-chemical-engineering/
Original file available at: http://dx.doi.org/10.1016/j.compchemeng.2013.10.003

Postprint version of paper published in Computers & Chemical Engineering, 2014, Volume 61 Pages38–50.
The content is identical to the published paper, but without the final typesetting by the publisher.

(Enhanced) Normalised Normal Constraint (ENNC) [17, 18]). From these sets the decision maker can select one point according to his/her preferences. Based on analytic relations [16, 19] the corresponding weights for a weighted sum implementation in the controller are derived. This approach has the advantage that a systematic representation of alternatives is possible while the traditional weighted sum formulation for the controller itself can still be used.

Moreover, the proposed procedure along with the cited works about multi-objective model predictive control strongly connects with the open field of economic (N)MPC. In particular, the proposed procedure also allows the DM to also optimally tune economic (N)MPC objectives.

The paper is structured as follows. Section 2 introduces the NMPC problem formulation. In Section 3 the systematic procedure at the core of this work is presented. In Section 4 the two case studies are introduced and consequently in Section 5 results are provided. Finally, Section 6 summarises the main conclusions.

2. NMPC with tracking objective formulation

In the classic NMPC formulation the objective function is most often obtained by combining different objective functions via a weighted sum approach. Moreover, when the NMPC is formulated as a tracking problem to a given reference its mathematical formulation is as follows:

$$\min_{\mathbf{u}(\tau)} J(\mathbf{x}(\tau), \mathbf{u}(\tau), t_\mathrm{c}, t_\mathrm{p}) \tag{1}$$

with:

$$J(\mathbf{x}(\tau), \mathbf{u}(\tau), t_\mathrm{c}, t_\mathrm{p}) = \int_t^{t+t_\mathrm{p}} F(\mathbf{x}(\tau), \mathbf{u}(\tau)) d\tau \tag{2}$$

$$F = (\mathbf{x} - \mathbf{x}_\mathrm{s})^\top Q (\mathbf{x} - \mathbf{x}_\mathrm{s}) + (\mathbf{u} - \mathbf{u}_\mathrm{s})^\top R (\mathbf{u} - \mathbf{u}_\mathrm{s}) \tag{3}$$

Journal homepage: http://www.journals.elsevier.com/computers-and-chemical-engineering/
Original file available at: http://dx.doi.org/10.1016/j.compchemeng.2013.10.003

Postprint version of paper published in Computers & Chemical Engineering, 2014, Volume 61 Pages38–50.
The content is identical to the published paper, but without the final typesetting by the publisher.

subject to:

$$\dot{\mathbf{x}}(\tau) = \mathbf{f}(\mathbf{x}(\tau), \mathbf{u}(\tau)), \forall\ \tau \in [t, t + t_\mathrm{p}] \tag{4}$$
$$\mathbf{u}(\tau) \in U, \forall\ \tau \in [t, t + t_\mathrm{c}] \tag{5}$$
$$\mathbf{u}(\tau) = \mathbf{u}(\tau + t_\mathrm{c}), \forall\ \tau \in [t + t_\mathrm{c}, t + t_\mathrm{p}] \tag{6}$$
$$\mathbf{x}(\tau) \in X, \forall\ \tau \in [t, t + t_\mathrm{p}] \tag{7}$$
$$\mathbf{x}(\tau) \in X_\mathrm{f}, \forall\ \tau \in [t, t + t_\mathrm{p}] \tag{8}$$

where $\dot{\mathbf{x}}$ represents the dynamic system in the form of Ordinary Differential Equations (ODEs), an extension to Differential Algebraic Equations (DAEs) is equally possible. Additionally, it was shown by [20, F.Manenti et al.] and [21, S. Dubljevic and P. D. Christofides] that the (N)MPC formulation can also be used for Partial Differential/Algebraic Equations (PDEs/PDAEs). $\mathbf{x}$ are the state variables, $\mathbf{u}$ are the control variables, t_c and t_p are respectively the control and prediction horizon. X_f represents the terminal set. Moreover, t is the independent variable within the NMPC algorithm while τ represents the process time. Finally, J is the objective function obtained via a Weighted Sum approach, in which Q and R are weight matrices. Nowadays, the selection of the weights that constitute the matrices Q and R is mainly done with an exhausting trail and error procedure or by following heuristic tuning procedures for linear MPC. This research aims at closing the gap by presenting a systematic procedure which is suitable for both linear and nonlinear MPC controllers.

3. NMPC Multi-Objective Tuning Procedure

The Multi-Objective Tuning Procedure (MOTP) that is introduced in this work consists of a multi-objective dynamic optimisation performed, when needed, in between the NMPC algorithm. The main application of the presented techniques results in the situation when the plant, subjected to the NMPC controller, is performing a planned transient from one operating point to a second known one. Hence, it can be assumed, for example, that an upper Real Time Optimisation (RTO) layer is present above the NMPC and feeds the controller with a new set-point to be tracked. Figure 1 displays a scheme of the procedure. At this point the MOTP is performed and a set of optimal control policies is returned to the decision maker (DM) (e.g., the responsible for the plant) who can choose among them. The decision step can also be performed within the procedure by introducing some a-priori knowledge on the

Journal homepage: http://www.journals.elsevier.com/computers-and-chemical-engineering/
Original file available at: http://dx.doi.org/10.1016/j.compchemeng.2013.10.003

preferences of the DM, for example the compromised solution can be selected (i.e., the point of the Pareto closest to the utopia point) or some limitation on the control action. The selected control policy in the form of a set of optimal weight matrices is then supplied to the NMPC controller. The MOTP step consists of solving an optimal control problem in which the mathematical formulation is identical to the one used for the NMPC algorithm implemented. In particular, the optimal control problem, has the same objective function of the NMPC, the sampling time equals the discretisation used in the off-line problem while the prediction horizon defines the final time. The MOTP is solved with advanced multi-objective methods and gives back a Pareto Front (PF) that illustrates the trade-offs between different control actions. Each of these control actions is returned with a weight matrix. Each weight matrix contains one weight for each single objective considered in the optimal control problem. All multi-objective problems and the NMPC controller are solved with the open source software ACADO toolkit [22, B. Houska et al. 2011].

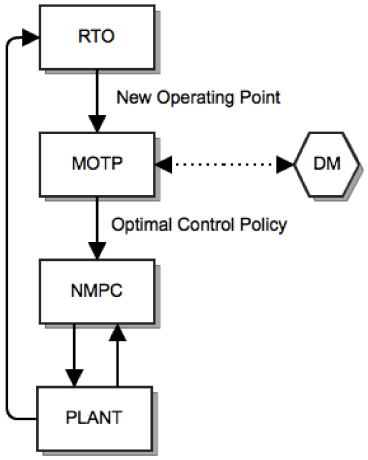

Figure 1: Schematic representation of the proposed multi-objective tuning procedure (MOTP). In the figure it is possible to identify the Decision Maker step (DM). This step can also be integrated in the MOTP via an a priori articulation of preferences.

Postprint version of paper published in Computers & Chemical Engineering, 2014, Volume 61 Pages38–50.
The content is identical to the published paper, but without the final typesetting by the publisher.

3.1. Multi-objective Optimisation

In this section the reader is introduced to Multi-Objective Optimisation Problems (MOOP) and the advanced methods that are the base of the systematic tuning procedure.

The general formulation of a multi-objective optimisation problem can be formulated as:

$$\min_{\mathbf{x}\in\mathbb{R}^n} \{J_1(\mathbf{x}), J_2(\mathbf{x}), \ldots, J_{\mathrm{m}}(\mathbf{x})\} \tag{9}$$

$$\text{subject to :} \quad \mathbf{g}(\mathbf{x}) \geq 0 \tag{10}$$

$$\mathbf{h}(\mathbf{x}) = 0 \tag{11}$$

with $m \geq 2$. Here, each $J_i(\mathbf{x})$ denotes an individual *objective function*, which are all grouped into the *cost vector* $\mathbf{J}(\mathbf{x}) = [J_1(\mathbf{x}), J_2(\mathbf{x}), \ldots, J_{\mathrm{m}}(\mathbf{x})]^\top$. The vector $\mathbf{g} = [g_1(\mathbf{x}), g_2(\mathbf{x}), \ldots, g_{n_{\mathrm{ineq}}}(\mathbf{x})]^\top : \mathbb{R}^n \to \mathbb{R}^{n_{\mathrm{ineq}}}$ and vector $\mathbf{h} = [h_1(\mathbf{x}), h_2(\mathbf{x}), \ldots, h_{n_{\mathrm{eq}}}(\mathbf{x})]^\top : \mathbb{R}^n \to \mathbb{R}^{n_{\mathrm{eqc}}}$ represent the *inequality* and *equality* constraints, respectively. Hence, the *feasible decision space* is $\mathcal{S} = \{\mathbf{x} : \mathbf{g}(\mathbf{x}) \leq 0 \text{ and } \mathbf{h}(\mathbf{x}) = 0\}$ and its mapping into the cost space yields the *feasible cost space* $\mathcal{J} = \{\mathbf{J}(\mathbf{x}) : \mathbf{x} \in \mathcal{S}\}$. In multi-objective optimisation typically no single solution exists. To determine a set of optimal solutions the concept of *Pareto optimality* is used.

Definition. A point $\mathbf{x}^* \in S$, is Pareto optimal iff there does not exist another point $\mathbf{x} \in S$, such that $J_i(\mathbf{x}) \leq J_i(\mathbf{x}^*)$ for all i and $J_j(\mathbf{x}) < J_j(\mathbf{x}^*)$ for at least one objective function j.

Furthermore, the following items are introduced, considering a minimization framework: the *minimizer* $\mathbf{x}_i^*$ of the i-th cost function $J_i(\mathbf{x})$, the *utopia point* $\mathbf{J}^* = [J_1^*, J_2^*, \ldots, J_m^*]^\intercal$ which contains the minima of the individual objective functions $J_i(\mathbf{x}_i^*)$, the *individual minima* cost vectors $\mathbf{J}(\mathbf{x}_i^*)$, which is the cost vector evaluated for the individual minimizer $\mathbf{x}_i^*$, the *nadir point* $\mathbf{J}^N = \max[J_1^N, J_2^N, \ldots, J_m^N]^\intercal$ which contains the worst value, for each objective, obtained from the *individual minima* cost vectors, the *pay-off* matrix $\mathbf{\Phi}$, whose i-th column is $\mathbf{J}(\mathbf{x}_i^*) - \mathbf{J}^*$, and the *Convex Hull of Individual Minima* CHIM which is defined as follows.

Definition. Given the *utopia point* $\mathbf{J}^*$ and the individual minima cost vectors $\mathbf{J}(\mathbf{x}_i^*)$, then the set of points in $\mathbb{R}^n$ that are a convex combination of $\mathbf{J}(\mathbf{x}_i^*) - \mathbf{J}^*$, *i.e.*, $\{\mathbf{\Phi w} \ : \ \mathbf{w} \in \mathbb{R}^n \ , \sum_{i=1}^m w_i, w_i \geq 0\}$, is referred to as the CHIM.

Journal homepage: http://www.journals.elsevier.com/computers-and-chemical-engineering/
Original file available at: http://dx.doi.org/10.1016/j.compchemeng.2013.10.003

Postprint version of paper published in Computers & Chemical Engineering, 2014, Volume 61 Pages38–50.
The content is identical to the published paper, but without the final typesetting by the publisher.

Finally, in order to obtain all the points of the Pareto set, a scalarisation approach is used in this case. The original multi-objective optimisation problem is converted in a parametric single objective optimisation problem. When this problem is solved for different values of the scalarisation parameters, a part of the Pareto front is obtained. In particular in this work the total number of single objective subproblems arising from the selected scalarisation method is given by the following formula:

$$\mathrm{N_p} = \frac{(m+p-2)!}{(m-1)!(p-2)!} \tag{12}$$

where $\mathrm{N_p}$ is the total number of single objective problems, m is the number of objective function considered and p is the number of single objective problems that the DM desired along one of the edges of the CHIM. In particular for a bi-objective problem $\mathrm{N_p} = p$. Several scalarisation methods exist in literature [8]. In the following subsections the scalarisation methods used in this work are presented.

3.1.1. Weighted Sum (WS).

As mentioned, the convex weighted sum is still the most often employed technique in practice:

$$\min_{\mathbf{x}\in S} J_{\mathrm{ws}} = \sum_{i=1}^{m} w_i J_i \text{ with } w_i \geq 0 \text{ and } \sum_{i=1}^{m} w_i = 1 \tag{13}$$

with $w_i \geq 0$ and $\sum_{i=1}^{m} w_i = 1$. Despite its simplicity, the weighted sum approach has several intrinsic drawbacks [15]. A uniform distribution of the weights does not necessarily results in an even spread on the Pareto front and points in non-convex parts of the Pareto set cannot be obtained.

3.1.2. Normal Boundary Intersection (NBI).

NBI reformulates the MOOP as follows [16]:

$$\max_{\mathbf{x}\in\mathcal{S},\lambda} \lambda \tag{14}$$

$$\text{subject to : } \mathbf{\Phi w} - \lambda \mathbf{\Phi e} = \mathbf{J}(\mathbf{x}) - \mathbf{J}^* \tag{15}$$

with $w_i \geq 0$ and $\sum_{i=1}^{m} w_i = 1$. Here $\mathbf{w}$ is the vector of scalarisation parameters, so called weights. Hence, $\mathbf{\Phi w}$ indicates a point on the hyperplane

Journal homepage: http://www.journals.elsevier.com/computers-and-chemical-engineering/
Original file available at: http://dx.doi.org/10.1016/j.compchemeng.2013.10.003

Postprint version of paper published in Computers & Chemical Engineering, 2014, Volume 61 Pages38–50.
The content is identical to the published paper, but without the final typesetting by the publisher.

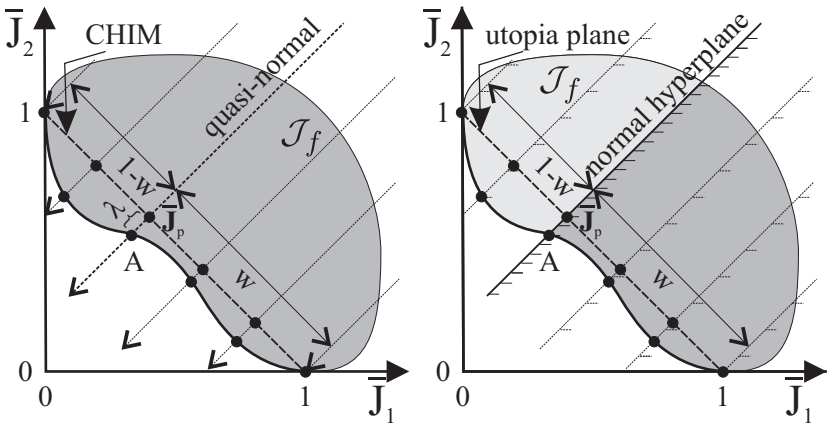

Figure 2: Schematic representation of NBI (left) and (E)NNC (right) for a bi-objective problem.

containing all individual minima and $-\lambda\mathbf{\Phi e}$ describes the (quasi-)normal direction to this plane. The plane is constructed by solving m single objective optimisation problems, where m is the number of objective considered in the MOOP. Each problem has as objective, one of the objectives considered alone and the solution of such a problem is called an *anchor point*. The *anchor points* constitute the vertices of the Convex-Hull of Individual Minima (CHIM). The rationale behind the method is that the intersection between the (quasi-)normal from any point $\mathbf{\Phi w}$ on the CHIM and the boundary of the feasible cost space closest to the utopia point is expected to be Pareto optimal. To this end, (14) introduces the maximisation of the length λ along the (quasi-)normal described by m additional equality constraints (15). A geometric interpretation of NBI for a bi-objective case is presented in Figure 2.

3.1.3. (Enhanced) Normalised Normal Constraint (ENNC).

ENNC reformulates the MOOP in an alternative way:

$$\min_{\mathbf{x}\in\mathcal{S}} \overline{J}_k \tag{16}$$

Journal homepage: http://www.journals.elsevier.com/computers-and-chemical-engineering/
Original file available at: http://dx.doi.org/10.1016/j.compchemeng.2013.10.003

Postprint version of paper published in Computers & Chemical Engineering, 2014, Volume 61 Pages38–50.
The content is identical to the published paper, but without the final typesetting by the publisher.

subject to:

$$(\overline{\mathbf{J}}(\mathbf{x}_k^*) - \overline{\mathbf{J}}(\mathbf{x}_i^*))^\top (\overline{\mathbf{J}}(\mathbf{x}) - \overline{\mathbf{J}}_\mathrm{p}) \leq 0 \qquad (17)$$
$$i = 1 \ldots m, i \neq k.$$

with $w_i \geq 0$ and $\sum_{i=1}^{m} w_i = 1$ as scalarisation parameters. Here, $\overline{\ }$ indicate normalised variables. The rationale is to minimise the single most important objective k (16), while reducing the feasible cost space by adding $m-1$ hyperplanes (17) that are orthogonal to the plane through the (normalised) individual minima. Normalisation can be achieved by first shifting the objectives such that the utopia point coincides with the origin and afterwards pre-multiplying them with a matrix $\mathbf{T}$:

$$\overline{\mathbf{J}}(\mathbf{x}) = \mathbf{T}(\mathbf{J}(\mathbf{x}) - \mathbf{J}^*). \qquad (18)$$

As Messac and Mattson [23] considered in the classic NNC only the shifting and scaling of the individual objectives, the matrix $\mathbf{T}$ is diagonal with as elements:

$$[\mathbf{T}]_{i,i} = \frac{1}{J_i^\square - J_i^*} \qquad (19)$$

where $J_i^\square = \max\{J_i(\mathbf{x}_j^*), j = 1, \ldots, m\}$ is the maximum for objective function i given the set of individual minimisers $\mathbf{x}_j^*$. In their ENNC, Sanchis et al. [18] introduce a different matrix $\mathbf{T}$ that can be generalized as follows:

$$\mathbf{T} = \mathbf{E}\mathbf{\Phi}^{-1} \qquad (20)$$

with $\mathbf{E}$ a matrix containing zeros on the diagonal and ones on the off-diagonal. As $\overline{\mathbf{\Phi}} = \mathbf{T}\mathbf{\Phi} = \mathbf{E}\mathbf{\Phi}^{-1}\mathbf{\Phi} = \mathbf{E}$, it is clear that the normalisation based on (20) maps the individual minima to the m vertices of an m-dimensional unit hypercube that each contain exactly one zero (see also Figure 2 for a geometric interpretation).

3.2. Analytic link between solutions of different scalarisation methods.

In order to appreciate the proposed tuning procedure the reader has to understand that scalarisation methods must in principle be able to generate the same Pareto optimal point. Therefore equivalence relations must exist that link a solution obtained with one method to settings of another method. It is possible to demonstrate that those links exist and their proofs are mainly

Journal homepage: http://www.journals.elsevier.com/computers-and-chemical-engineering/
Original file available at: http://dx.doi.org/10.1016/j.compchemeng.2013.10.003

Postprint version of paper published in Computers & Chemical Engineering, 2014, Volume 61 Pages38–50.
The content is identical to the published paper, but without the final typesetting by the publisher.

based on on showing that the different scalarisation reformulations give rise to identical stationary points, i.e., solutions satisfying the first-order optimality or Karush-Kuhn-Tucker conditions. For sake of brevity the proofs are not reported in this paper but can be found in [16, I. Das & J. Dennis, 1998] and [19, F. Logist & J. Van Impe]. Moreover, the last work presents that a stationary point obtained with the ENNC method can be analyticly linked to a solution of the WS (i.e., the weight matrix leading to the same solution). This analytic link will be exploited in the proposed procedure to obtain the optimal weight matrix for the NMPC.

3.2.1. From ENNC to NBI

Provided that the additional ENNC inequality constraints are active, ENNC and NBI yield a same stationary point $\mathbf{x}^*_{\text{NBI}} = \mathbf{x}^*_{\text{ENNC}}$ and related Lagrange multipliers:

$$\boldsymbol{\lambda}^*_{\text{NBI}} = \frac{1}{m-1}\overline{\boldsymbol{\lambda}}^*_{\text{ENNC}} \tag{21}$$

$$\boldsymbol{\mu}^*_{\text{NBI}} = \frac{1}{m-1}\overline{\boldsymbol{\mu}}^*_{\text{ENNC}} \tag{22}$$

$$\left(\mathbf{T}^{-1}\right)^{\top}\begin{bmatrix} \nu^*_{\text{NBI},1} \\ \vdots \\ \nu^*_{\text{NBI},m-1} \\ \nu^*_{\text{NBI},m} \end{bmatrix} = \frac{1}{m-1}\begin{bmatrix} \overline{\nu}^*_{\text{ENNC},1} \\ \vdots \\ \overline{\nu}^*_{\text{ENNC},m-1} \\ 1-\sum_{i=1}^{m-1}\overline{\nu}^*_{\text{ENNC},i} \end{bmatrix} \tag{23}$$

where $\boldsymbol{\lambda}^*_{\text{NBI}}$ are the Lagrange multipliers for the inequality constraints and $\boldsymbol{\mu}^*_{\text{NBI}}$ the ones for the equality constraints present in the original MOOP formulation, while $\boldsymbol{\nu}^*_{\text{NBI}}$ are the multipliers for the additional constraints defined during the scalarisation of the MOOP by the NBI method. In the same way, $\overline{\boldsymbol{\lambda}}^*_{\text{ENNC}}$ and $\overline{\boldsymbol{\mu}}^*_{\text{ENNC}}$ are the multipliers for the inequality and equality constraints present in the original MOOP while $\overline{\boldsymbol{\nu}}^*_{\text{ENNC}}$ are the additional inequality constraints imposed by the ENNC method.

Journal homepage: http://www.journals.elsevier.com/computers-and-chemical-engineering/
Original file available at: http://dx.doi.org/10.1016/j.compchemeng.2013.10.003

Postprint version of paper published in Computers & Chemical Engineering, 2014, Volume 61 Pages38–50.
The content is identical to the published paper, but without the final typesetting by the publisher.

3.2.2. From NBI to WS

Equation (23) allows making the connection from ENNC to the corresponding weights $w_{\mathrm{WS},i}$ of a WS via [16]:

$$w_{\mathrm{WS},i} = \frac{\nu^*_{\mathrm{NBI},i}}{\sum_{i=1}^{m} \nu^*_{\mathrm{NBI},i}}. \tag{24}$$

Hence, the weight matrix for the classic WS approach is obtained. Applying this weight matrix will steer the optimisation problem towards the same stationary points obtained with the advanced methods.

3.3. Software: ACADO Multi-Objective

ACADO Multi-Objective is an extension of the ACADO toolkit for automatic control and dynamic optimisation with all the multi-objective approaches presented above and successfully applied to optimal control problems [24, F. Logist et al.]. Due to the self contained object-oriented, C++ implementation, the toolkit (i) is easy-to-use, (ii) does not require third-party software, and (iii) allows a flexible control over algorithmic settings. Moreover, ACADO Multi-Objective presents several features to efficiently tackle multi-objective optimal control problems and that are going to be exploited for the systematic tuning procedure for (N)MPC presented in this work. The software is available open source at www.acadotoolkit.com.

4. Case studies

The procedure to systematically tune (N)MPC controller presented in this article is tested on two case studies: the Van de Vusse reactor and the Tennessee Eastman plant. While the former is a known benchmark application for nonlinear optimisation algorithms, the latter represents a challenging application to test on-line control strategies. Both cases have been extensively studied and a significant number of scientific works were based on them. In particular a description of the two mathematical models can be found in, e.g., [25, J. Bonilla Alarcon et al., 2010] for the Van de Vusse reactor and in, e.g., [26, J.J. Downs & E. F. Vogel, 1993] and [27, Jockenhövel et al., 2003] for the Tennessee Eastman plant. The two case studies cover a wide range of possible scenarios arising in on-line controls problems, e.g., presence of disturbances, model mismatch, presence of regularisation terms in the objective function.

Journal homepage: http://www.journals.elsevier.com/computers-and-chemical-engineering/
Original file available at: http://dx.doi.org/10.1016/j.compchemeng.2013.10.003

Postprint version of paper published in Computers & Chemical Engineering, 2014, Volume 61 Pages38–50.
The content is identical to the published paper, but without the final typesetting by the publisher.

4.1. Case Study I: Van de Vusse reactor

The Van de Vusse reactor is a well known benchmark example for (N)MPC and it consists of a continuous stirred tank reactor in which an exothermal reaction takes place. The reaction scheme is as follows:

$$\begin{aligned} &\mathrm{A} \xrightarrow{k_1} \mathrm{B} \xrightarrow{k_2} \mathrm{C} \\ &2\mathrm{A} \xrightarrow{k_3} \mathrm{D} \end{aligned} \tag{25}$$

The above reactions are exothermic and the heat generated needs to be removed from the reactor through an external jacket. The key point of this reactor is to maximise the production of B while maintaining a safe operation. Taking into consideration these aspects it is possible to write the following nonlinear system of ordinary differential equations that describe the behaviour of the reactor:

$$\frac{dC_a}{dt} = \frac{V}{V_r}(C_{a0} - C_a) - k_1 C_a - k_3 C_a^2 \tag{26}$$

$$\frac{dC_b}{dt} = \frac{V}{V_r}(-C_b) + k_1 C_a - k_2 C_b \tag{27}$$

$$\frac{dC_c}{dt} = \frac{V}{V_r}(-C_c) + k_2 C_b \tag{28}$$

$$\frac{dT}{dt} = \frac{V}{V_r}(T_0 - T) + \frac{k_w A_r}{\rho C_p V_r}(Tk - T) - \frac{1}{\rho C_p}(R_1 + R_2 + R_3) \tag{29}$$

$$\frac{dT_k}{dt} = \frac{1}{m_k C_{pk}}(Q_k + k_w A_r (T_k - T)) \tag{30}$$

where C_a, C_b, C_c are the concentrations of reactant A, product B and unwanted by-product C, k_i are the reaction rates depending on temperature T via an Arrhenius law, R_i are the heats generated by each reaction. V and V_r are the reactant flow rate and reaction volume. $\frac{V}{V_r}$ and Q_k, the heat removal rate, are the two control variables. ρ is the solution density, A_r and k_w are the surface and the heat transfer coefficient for the cooling jacket, m_k is the coolant flow rate, C_p and C_{pk} denote the heat capacity of the reaction solution and coolant, T_k is the coolant temperature. Values used to initialise the problem respectively are: $C_a = 2.14\frac{\mathrm{mol}}{\mathrm{l}}$, $C_b = 1.09\frac{\mathrm{mol}}{\mathrm{l}}$, $C_c = 1.10\frac{\mathrm{mol}}{\mathrm{l}}$, $T = 114.2°\mathrm{C}$ and $T_k = 112.9°\mathrm{C}$. Moreover, the system is subject to several constraints:

Journal homepage: http://www.journals.elsevier.com/computers-and-chemical-engineering/
Original file available at: http://dx.doi.org/10.1016/j.compchemeng.2013.10.003

Postprint version of paper published in Computers & Chemical Engineering, 2014, Volume 61 Pages38–50.
The content is identical to the published paper, but without the final typesetting by the publisher.

$$C_i \geq 0.0, \text{ with } i = a, b, c. \tag{31}$$

$$3.0 \leq \frac{V}{V_r} \leq 35.0 \tag{32}$$

$$-9000.0 \leq Q_k \leq 0.0 \tag{33}$$

It has to be noted that in this work, the classic model reported in literature has been extended with an additional differential state to explicitly account for the unwanted by-product C. This was done in order enable a tracking term for both the product B and the by-product C in the objective function. Hence, it is possible to write two objective functions. In particular, the terms J_{B} for tracking the concentration of B and J_{C} for tracking the concentration of C can be written as follows:

$$J_{\mathrm{B}} = (C_b - C_{bs})^\top w_1 (C_b - C_{bs}) \tag{34}$$

$$J_{\mathrm{C}} = (C_c - C_{cs})^\top w_2 (C_c - C_{cs}) \tag{35}$$

When these two terms are combined a global objective unction is obtained:

$$J = (\mathbf{C} - \mathbf{C}_s)^\top Q_{\mathrm{vdv}} (\mathbf{C} - \mathbf{C}_s) \tag{36}$$

where $\mathbf{C}$ and $\mathbf{C}_s$ respectively identify the vector of the states and the vector containing the reference set-points, while the matrix Q_{vdv} represent the weight matrix for this application. In particular, the two vectors and the matrix can be written as:

$$\mathbf{C} = \begin{bmatrix} C_b \\ C_c \end{bmatrix} \quad \mathbf{C_s} = \begin{bmatrix} C_{bs} \\ C_{cs} \end{bmatrix} \tag{37}$$

$$Q_{\mathrm{vdv}} = \begin{bmatrix} w_1 & 0 \\ 0 & w_2 \end{bmatrix} \tag{38}$$

The aim of the systematic tuning procedure will be to present to the decision maker a set of possible weights w_1 and w_2 from which he/she can pick one according to his/her preferences and that will determine the tracking policy of the controller.

Journal homepage: http://www.journals.elsevier.com/computers-and-chemical-engineering/
Original file available at: http://dx.doi.org/10.1016/j.compchemeng.2013.10.003

Postprint version of paper published in Computers & Chemical Engineering, 2014, Volume 61 Pages38–50.
The content is identical to the published paper, but without the final typesetting by the publisher.

4.2. Case Study II: Tennessee Eastman Plant

The second case study concerns the Tennessee Eastman plant. For this work the model of the whole plant has been reduced and only the mixing zone and the nonlinear reactor are taken in consideration. This reduction was already proposed in literature see references within [27, Jockenhövel et al., 2003]. The resulting model still represents a considerable challenge and a more then realistic test case for the proposed procedure presented for two reasons. First, the main nonlinearities in the model of the plant are given by the double phase reactor and the number of differential and algebraic states is only partially reduced accounting respectively for 18 differential and 64 algebraic states. In particular the system of equations arises from the following reaction scheme:

$$\begin{aligned} &A_{(g)} + C_{(g)} + D_{(g)} \rightarrow G_{(liq)} \\ &A_{(g)} + C_{(g)} + E_{(g)} \rightarrow H_{(liq)} \\ &A_{(g)} + E_{(g)} \rightarrow F_{(liq)} \\ &3D_{(g)} \rightarrow 2F_{(liq)} \end{aligned} \tag{39}$$

All reactions are exothermic and irreversible. The kinetic constants depend on the concentration of the reactants in the reactor gas phase and on the temperature via an Arrhenius expression. The reactants A, C, D, E react with each other in the gas phase to produce the two products G and H and a by-product F in the liquid phase. Additionally, an inert component B that has the function of solvent is present. The plant as a whole consists of five main units: the reactor, the condenser, the vapor-liquid separator, the recycle compressor and the final stripper unit to obtain the final products. As mentioned above the method proposed in this paper is applied at the reactor unit and the mixing zone in which the fresh reactant are mixed with the recycle stream. The resulting stream is fed to the reactor in which the exothermic reactions take place. It has to be noted that the composition and amount of the recycle stream is kept constant for the simulations in this work. Moreover, it can be eventually considered as a disturbance for further studies. Accounting for mass and enthalpy balances for the mixing zone and the reactor enables writing the system of differential algebraic equations:

The molar balances for the components A-H in the mixing zone can be

Journal homepage: http://www.journals.elsevier.com/computers-and-chemical-engineering/
Original file available at: http://dx.doi.org/10.1016/j.compchemeng.2013.10.003

Postprint version of paper published in Computers & Chemical Engineering, 2014, Volume 61 Pages38–50.
The content is identical to the published paper, but without the final typesetting by the publisher.

written as:

$$\frac{dN_{i,m}}{dt} = y_{i,1}F_1 + y_{i,2}F_2 + y_{i,3}F_3 + y_{i,5}F_5 + y_{i,8}F_8 - y_{i,6}F_6 \quad (40)$$

Hence, the energy balances arising in the mixing zone are:

$$\left(\sum_{i=\mathrm{A}}^{\mathrm{H}} N_{i,m}c_{p,\mathrm{vap},i}\right)\frac{dT_m}{dt} = \sum_{j=1,2,3,5,8} F_j\left(\sum_{i=A}^{\mathrm{H}} y_{i,j}c_{p,\mathrm{vap},i}\right)(T_j - T_m) \quad (41)$$

$$y_{i,6} = \frac{N_{i,m}}{\sum_{j=\mathrm{A}}^{\mathrm{H}} N_{j,m}} \quad (42)$$

$$p_m = \sum_{i=\mathrm{A}}^{\mathrm{H}} N_{i,m}\frac{RT_m}{V_m} \quad (43)$$

In the same way the molar balances for the components in the reactor are represented by:

$$\frac{dN_{i,m}}{dt} = y_{i,6}F_6 - y_{i,7}F_7 + \sum_{j=1}^{3}\nu_{ij}R_j \text{ for } i = \mathrm{A}, ..., \mathrm{H} \quad (44)$$

Therefore the resulting energy balances for the reactor are described as:

$$\left(\sum_{i=\mathrm{A}}^{\mathrm{H}} N_{i,r}c_{p,\mathrm{vap},i}\right)\frac{dT_r}{dt} = F_6\left(\sum_{i=\mathrm{A}}^{\mathrm{H}} y_{i,6}c_{p,\mathrm{vap},i}\right)(T_6 - T_r) - \dot{Q}_r - \sum_{j=1}^{3}\Delta H_{Rj}R_j \quad (45)$$

Where the term ΔH_{Rj} is defined as follows:

$$\Delta H_{Rj} = \sum_{i=\mathrm{A}}^{\mathrm{H}} H_i\nu_{i,j} + HOF_j;\ H_i = c_{p,i}\,(T_r - T^*) \quad (46)$$

A significant difference with the mixing zone is due to the chemical reactions taking place in the reactor, these can be mathematically expressed through the reaction kinetics:

$$R_1 = \alpha_1 V_{V,r}\exp\left[44.06 - \frac{42600}{RT_r}\right]p_{A,r}^{1.08}\ p_{C,r}^{0.311}\ p_{D,r}^{0.874} \quad (47)$$

$$R_2 = \alpha_2 V_{V,r}\exp\left[10.27 - \frac{19500}{RT_r}\right]p_{A,r}^{1.15}\ p_{C,r}^{0.370}\ p_{E,r}^{1.00} \quad (48)$$

$$R_3 = \alpha_3 V_{V,r}\exp\left[59.50 - \frac{59500}{RT_r}\right]p_{A,r}\,(0.77\ p_{D,r} + p_{E,r}) \quad (49)$$

Journal homepage: http://www.journals.elsevier.com/computers-and-chemical-engineering/
Original file available at: http://dx.doi.org/10.1016/j.compchemeng.2013.10.003

Postprint version of paper published in Computers & Chemical Engineering, 2014, Volume 61 Pages38–50.
The content is identical to the published paper, but without the final typesetting by the publisher.

The reactor input and output flows are:

$$F_6 = 0.8334 \frac{\text{kmol}}{\text{s}\sqrt{\text{MPa}}} \sqrt{p_m - p_r} \quad (50)$$

$$F_7 = 1.5355 \frac{\text{kmol}}{\text{s}\sqrt{\text{MPa}}} \sqrt{p_r - p_s} \quad (51)$$

Due to the exothermic reactions a cooling jacket is needed and the heat exchanged can be calculated as:

$$\dot{Q}_r = m_{CW,r}\ c_{p,CW}\ \left(T_{CW,r,\text{out}} - T_{CW,r,\text{in}}\right) \quad (52)$$

$$\dot{Q}_r = UA_r \left(\frac{\Delta T_1 - \Delta T_2}{\ln \Delta T_1 / \Delta T_2} \right) \quad (53)$$

$$\Delta T_1 = T_r - T_{CW,r,\text{in}} \quad (54)$$

$$\Delta T_2 = T_r - T_{CW,r,\text{out}} \quad (55)$$

Finally, since inside the reactor a two phase mixture is present, the vapor-liquid equilibrium needs to be introduced as follows:

$$p_{i,r} = \gamma_{i,r}\ xi, r\ p_{i,r}^{sat}\left(T_r\right)\ \ i = \text{D}, ..., \text{H} \quad (56)$$

$$p_{i,r} = \frac{N_{i,r,\text{vap}}\ RT_{,r}}{V_{V,r}}\ \ i = \text{A}, \text{B}, \text{C} \quad (57)$$

$$p_{i,r}^{\text{sat}}\left(T\right) = 10^{-3} \exp\left[A_i + \frac{B_i}{C_i + T_r - T^*}\right]\ \ i = \text{D}, ..., \text{H} \quad (58)$$

$$p_r = \sum_{i=\text{A}}^{\text{H}} p_{i,r} \quad (59)$$

$$y_{i,7} = \frac{p_{i,r}}{p_r}\ \ i = \text{A}, ..., \text{H} \quad (60)$$

$$x_{i,r} = \frac{N_{i,r}}{\sum_{i=\text{D}}^{\text{H}} N_{i,r}}\ \ i = \text{D}, ..., \text{H} \quad (61)$$

$$V_{L,r} = \frac{\sum_{i=\text{D}}^{\text{H}} N_{i,r,\text{liq}}}{\rho_{\text{liq},r}}\ V_{V,r} = V_r - V_{L,r} \quad (62)$$

The model has been adapted from the version reported in [27, Jockenhövel et al.]. In the current version the PID controllers are not implemented.

Journal homepage: http://www.journals.elsevier.com/computers-and-chemical-engineering/
Original file available at: http://dx.doi.org/10.1016/j.compchemeng.2013.10.003

Postprint version of paper published in Computers & Chemical Engineering, 2014, Volume 61 Pages38–50.
The content is identical to the published paper, but without the final typesetting by the publisher.

Therefore it results in a more challenging control problem as the system is now open-loop unstable.

Having introduced the case study in general, it allows to describe the detail of the implementation used in this work. In particular, since only the reactor unit is considered in this work the objective function is defined in order to control the behaviour of this unit. Hence, temperature and pressure inside the reactor are tracked along with a regularisation term that takes into account the flows entering in the reactor and the flow of cooling water to the jacket. This translates in the following objective function:

$$J = (\mathbf{x} - \mathbf{x}_s)^\top Q_{\mathrm{TE}}(\mathbf{x} - \mathbf{x}_s) + (\mathbf{u} - \mathbf{u}_s)^\top R_{\mathrm{TE}}(\mathbf{u} - \mathbf{u}_s) \tag{63}$$

in which $\mathbf{x}$ and $\mathbf{x_s}$ are respectively the vector of the states and the vector of set points for the two states. In the same way $\mathbf{U}$ and $\mathbf{U_s}$ are the vectors of manipulated variables and their set points used in the regularisation term.

$$\mathbf{X} = \begin{bmatrix} P \\ T \end{bmatrix}, \ \mathbf{X_s} = \begin{bmatrix} P_s \\ T_s \end{bmatrix} \tag{64}$$

$$\mathbf{U} = \begin{bmatrix} m_{cw} \\ F_1 \\ F_2 \\ F_3 \end{bmatrix}, \ \mathbf{U_s} = \begin{bmatrix} m_{cws} \\ F_{1s} \\ F_{2s} \\ F_{3s} \end{bmatrix} \tag{65}$$

Moreover, the above objective function was reformulated into two clearly distinguished objective functions, as follows:

$$J_P = (P - P_s)^\top w_1 (P - P_s) + (\mathbf{U} - \mathbf{U_s})^\top \frac{R_{\mathrm{TE}}}{2} (\mathbf{U} - \mathbf{U_s}) \tag{66}$$

$$J_T = (T - T_s)^\top w_2 (T - T_s) + (\mathbf{U} - \mathbf{U_s})^\top \frac{R_{\mathrm{TE}}}{2} (\mathbf{U} - \mathbf{U_s}) \tag{67}$$

This reformulation allows the regularisation term to be directly introduced in each of the two objectives. In particular, the value of the weight for the regularisation term was fixed at $R_{\mathrm{TE}} = 0.01$. When formulating the NMPC objective function the two equations above are going to be summed to each other, hence, the division of R_{TE} by two. The weight matrix R_{TE} is assumed to be constant and composed by a single element w_3. Given this, it is possible to write the two separate weight matrices as follows:

Journal homepage: http://www.journals.elsevier.com/computers-and-chemical-engineering/
Original file available at: http://dx.doi.org/10.1016/j.compchemeng.2013.10.003

Postprint version of paper published in Computers & Chemical Engineering, 2014, Volume 61 Pages38–50.
The content is identical to the published paper, but without the final typesetting by the publisher.

Case Study I: Van de Vusse reactor			
MOTP		NMPC	
Final Time	2000 s	Prediction Horizon (HP)	2000 s
		Control Horizon (HC)	2000 s
Control Discretisation	50	Control Discretisation	50
Simulated Time	2000 s	Simulated Time	4000 s

Table 1: Settings used for the MOTP and the NMPC for Case Study I: Van de Vusse reactor

$$Q_{\mathrm{TE}} = \begin{bmatrix} w_1 & 0.0 \\ 0.0 & w_2 \end{bmatrix} \tag{68}$$

$$R_{\mathrm{TE}} = w_3 = 0.01 \tag{69}$$

In this case study the MOTP will return the weight matrices Q_{TE}. A particular aspect to be considered for this application is that a unique coefficient is assigned as a weight for all manipulated variable in the regularisation term. Hence, weights w_1, w_2 and w_3 are the weights for the pressure, the temperature and the manipulated variables respectively.

5. Results

In this section the results obtained from the multi-objective optimisations in the MOTP steps and the NMPC are presented. Table 1 and Table 2 report the settings used for the solution of the MOTP and NMPC for Case Study I: Van de Vusse reactor and Case Study II: Tennessee Eastman plant.

In particular, the settings in Table 1 have to be interpreted as follows. For the offline problem (MOTP) a time window (final time) of 2000 s is adopted. In this time window an optimal control profile has be found that is discretised in 50 piecewise constant elements of equal length. Hence, one control element corresponds to 40 s. As the offline problem is solved only once without shifting the time window, the simulated time equals the final time.

Journal homepage: http://www.journals.elsevier.com/computers-and-chemical-engineering/
Original file available at: http://dx.doi.org/10.1016/j.compchemeng.2013.10.003

Postprint version of paper published in Computers & Chemical Engineering, 2014, Volume 61 Pages38–50.
The content is identical to the published paper, but without the final typesetting by the publisher.

Case Study II: Tennessee Eastman plant			
MOTP		NMPC	
Final Time	7200 s	Prediction Horizon (HP)	7200 s
		Control Horizon (HC)	7200 s
Control Discretisation	72	Control Discretisation	72
Simulated Time	7200 s	Simulated Time	36000 s

Table 2: Settings used for the MOTP and the NMPC for Case Study II: Tennessee Eastman plant

In contrast, for the online problem (NMPC) a moving time window of 2000 s (prediction horizon HP) is used and the total simulated time is 4000 s. In order to achieve a similar control accuracy, the control horizon HC equals the prediction horizon HP (i.e., 2000 s) and also a piecewise constant control discretisation with 50 elements of equal length is employed. Hence, the length of the control element in the NMPC is equal to the length used in the MOTP, i.e., 40 s. The settings in Table 2 have a similar interpretation.

5.1. Case Study I: Van de Vusse Reactor

For this case study also the RTO step is solved via a multi-objective steady-state optimisation. In Figure 3, the PF obtained for the multi-objective steady-state problem is visualised. Every point in Figure 3 represents a steady-state operation point for the reactor. Hence, it is possible for the decision maker to select the preferred operating point for the reactor. For this work the point represented by $\square$ is chosen as the new operating point. Therefore, the MOTP step is fed with the new operating point and takes care of solving a dynamic multi-objective optimisation with a tracking objective function. The solution of this problem is a PF in which each point represents an optimal control policy. Therefore, any of the optimal control policies will guide the reactor from the starting steady-state condition, identified by $\triangle$ to the new one indicated by $\square$. It is worth pointing out that the procedure can be applied to any tracking problem, moving from one point in the set to another.

Figure 4 reports the results obtained in the MOTP step. The two PFs are respectively achieved with the classic WS (left graph) and the ENNC method (right graph). In particular, both graphs are obtained by scalarisation of the

Journal homepage: http://www.journals.elsevier.com/computers-and-chemical-engineering/
Original file available at: http://dx.doi.org/10.1016/j.compchemeng.2013.10.003

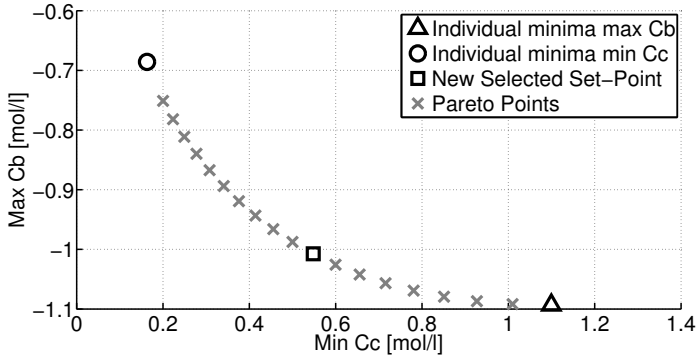

Figure 3: Pareto Front of steady-state solutions for the Van de Vusse reactor. It was obtained with the ENNC method and a filter to remove dominated points was applied. Each of these points can be fed to the MOTP step in order to calculate the optimal tracking policy to drive the system to the new operating conditions.

original multi-objective problem with the same uniform set of scalarisation parameters.

The left graph in Figure 5 illustrates the evenly distributed set of scalarisation parameters. However, from the comparison between the two graphs, it is possible to appreciate that the WS does not deliver a uniform set of Pareto points. Hence, in the WS case a fixed variation of the scalarisation parameters does not correspond to a proportional change on the results obtained. On the other hand, the Pareto front obtained with the ENNC method appears to be evenly spread.

Moreover, if the maximum distance between two consecutive points on a PF is taken as a measure of accuracy, it can be seen how the PF obtained with the WS approach exhibits a lack of accuracy in at least one region of the front (i.e. in the neighborhood of the anchor point ○). On the contrary, the PF obtained with the ENNC shows the same level of accuracy on the whole front. Hence, the ENNC guarantees a systematic accuracy on the obtained PF, while with the WS approach this kind of accuracy is hardly achievable. This last statement holds for the WS unless a considerable number of subproblems is solved.

However, as presented in Section 3.2 it is possible to obtain a set of

Journal homepage: http://www.journals.elsevier.com/computers-and-chemical-engineering/
Original file available at: http://dx.doi.org/10.1016/j.compchemeng.2013.10.003

Postprint version of paper published in Computers & Chemical Engineering, 2014, Volume 61 Pages38–50.
The content is identical to the published paper, but without the final typesetting by the publisher.

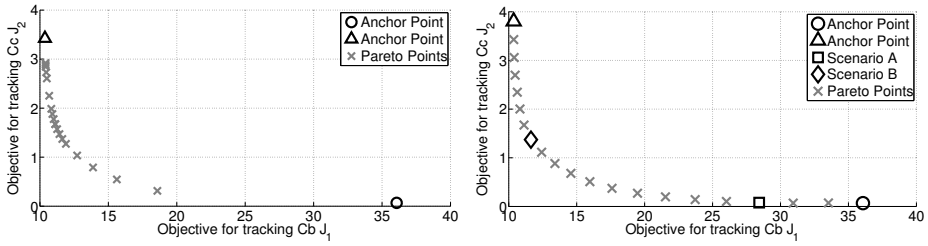

Figure 4: The left graph represents the PF obtained in the MOTP step using the classic WS algorithm, while the right one depicts the PF front obtained in the MOTP step using the ENNC methods. Both methods used a uniform spread of weights.

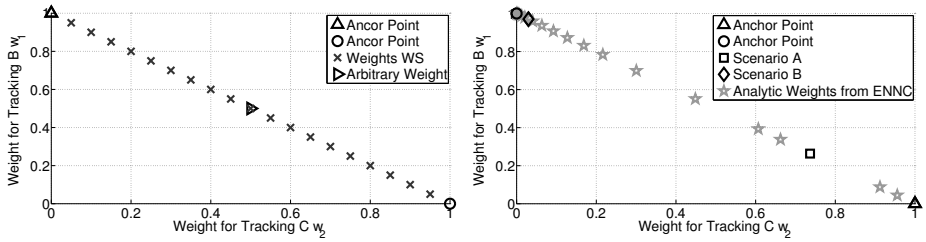

Figure 5: Set of weights used for the classic scalarisation of the WS approach (left graph) against the weights for the WS obtained from the ENNC method through the analytic relations (right graph).

weights that causes the WS to reproduce the Pareto set obtained with the ENNC method. The right graph in Figure 5 illustrates the set of weights obtained by applying the analytic relation. It is possible to appreciate that the set of weights obtained through the analytic relations are quite different from the evenly spread ones normally used in the WS method (compare the two graphs in Figure 5). This difference represents in a nutshell why the selection of weights for a WS objective function is far from easy.

In order to make this concept more clear, the two points identified with □ and ◇ of the right graph in Figure 4 are selected. These two points correspond to two weight matrices □ and ◇ (right graph in Figure 5) and are then used to perform two different scenarios in the NMPC, i.e., Scenario A and B. Scenario A (SA) uses a weight matrix Q that leads to a better tracking of C_c ($w_1 = 0.263$ and $w_2 = 0.737$) and Scenario B (SB) employs one that allows a better tracking of C_b ($w_1 = 0.969$ and $w_2 = 0.041$). These scenarios are

Journal homepage: http://www.journals.elsevier.com/computers-and-chemical-engineering/
Original file available at: http://dx.doi.org/10.1016/j.compchemeng.2013.10.003

compared to the one using an arbitrary weight (AW) matrix Q, i.e., $w_1 = 0.5$ and $w_2 = 0.5$.

Since the selected weights are exactly the same for the two objectives, the resulting tracking policy is expected to be equally focused on at the control of both concentrations. However, it is already possible to predict what will be the true output of the simulation performed with arbitrary weights by considering the position of a point with coordinates (0.5,0.5) in the set of weights depicted in the right graph in Figure 5. In fact, it can be seen how the point identified by the arbitrary weights lies closer to the point identified by □. Hence, the control policy adopted by the system when the arbitrary weights are used will be, as it will be shown, similar to the one obtained by the weight matrix used in Scenario A. Once again, this behaviour could have only been identified with a series of trials that would have taken a considerable amount of time. On the other hand, the solution obtained by the proposed procedure concentrates in one graph all the information needed to select an appropriate weight matrix.

Figure 6 depicts the different responses of the plant when it is subjected to the different weight matrices introduced above. In particular, it is possible to appreciate that the weight matrix identified as Scenario B causes the NMPC to have a tight control on the concentration of the product B, while the weights used in the Scenario A cause the NMPC to control more accurately the concentration of the by-product C. Obviously, the cause of these different behaviours lies in the discrepancy between the control actions (Figure 7), used by the NMPC controller.

As a measure of the effect caused by the different weight matrices adopted the integral of the absolute value of the difference between the curves is introduced. Table 3 summarises the values obtained with this method. In particular, the left part of Table 3 refers to the left graph in Figure 6, while the right part of the same table refers to the right graph. Moreover, the curve the curve identified as SB is taken as a reference for the left part of the table and the curve denoted by SA is selected as a reference for the right part of the table. Hence, the values in the left part of Table 3 correspond to the integrals of absolute value of the difference between the curve obtained with arbitrary weights (AW) and the curve obtained with weights for SA from the reference SB in the left graph in Figure 6. In the same way, the right part

Postprint version of paper published in Computers & Chemical Engineering, 2014, Volume 61 Pages38–50.
The content is identical to the published paper, but without the final typesetting by the publisher.

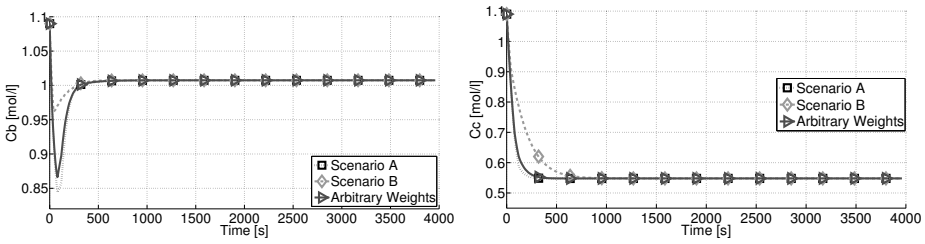

Figure 6: The two graphs reported represent the behaviour of the plant when subjected to the different weight matrices identified by the two scenarios A and B compared to the behaviour of the plant when the weights are arbitrarily selected. The left graph shows the trend followed by the concentration of product B, while the right one shows the trend for the concentration of by-product C.

of Table 3 reports the values of the integrals of the absolute values of the difference between the curve characterized by arbitrary weights (AW) and the curve represented by SB from the reference SA.

From the two graphs in Figure 6 and the values reported in Table 3 it is clear that the system responds in a similar way when subjected to a NMPC controller defined with the weight matrix AW and the weight matrix SA. On the other hand, the response of the system appears to be significantly different when the NMPC controller is defined by the weight matrix SB. This result is in line with what was expected from the analysis made based on the set of weight matrices obtained from the MOTP procedure (right graph of Figure 5).

The benefit of applying the proposed procedure for the selection of the weight matrix for the objective function for a NMPC controller is remarkable. In particular, the reader has to consider how cumbersome and time consuming it could have been to have the system respond according to his/her preferences by adopting a trial and error procedure for tuning the weight matrix. On the other hand, the result of the MOTP concentrates in one graph all the information needed by the practitioner to perform his/her choice.

5.2. Reliability of the controller

The Van de Vusse Reactor case study was used to test the reliability of the proposed procedure and the used NMPC controller under different possible scenarios arising in on-line control problems, e.g., presence of disturbances,

Journal homepage: http://www.journals.elsevier.com/computers-and-chemical-engineering/
Original file available at: http://dx.doi.org/10.1016/j.compchemeng.2013.10.003

Postprint version of paper published in Computers & Chemical Engineering, 2014, Volume 61 Pages38–50.
The content is identical to the published paper, but without the final typesetting by the publisher.

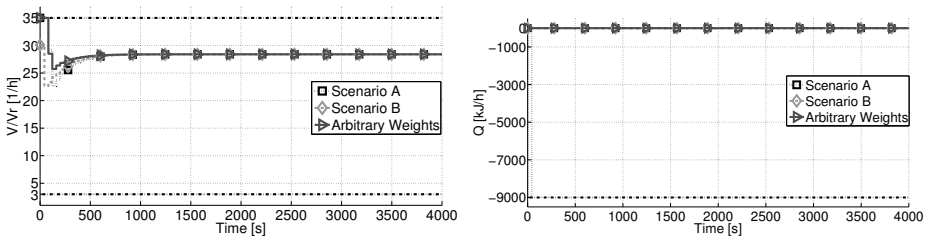

Figure 7: The two graphs reported highlight the differences in control action used by the NMPC to control the plant when subjected to the different sets of weight matrices identified by the two scenarios A and B compared to the behaviour of the plant when the weights are arbitrarily selected. The left graph depicts the control action for the inlet flow, while the right one displays the action for the duty in the jacket.

Integrated Absolute Difference			
Concentration of B		Concentration of C	
SB - AW	12.44	SA - AW	4.88
SB - SA	17.53	SA - SB	54.11

Table 3: Difference between trends followed by the state variables for both graphs in Figure 6. The reported numbers represent the integral of the absolute values of the difference between the curves.

model mismatch and different settings for the controller. In particular, it has to be noted that no discussion about the stability of the (N)MPC controller is reported in this work for the sake of brevity. The reason for this is that a classic (N)MPC controller with the real-time algorithm scheme introduced in [3, M. Diehl et.al] is used. A proof of the stability of such (N)MPC controller can be found in the referenced paper. Moreover, the effect of different prediction horizon lengths is evaluated in the next section.

5.2.1. Influence of Prediction Horizon Length

One aspect that should be considered is the impact of the proposed procedure on the design of the controller itself, i.e., how changing important parameters such as the length of the prediction horizon will effect the response of the controller. Figure 8 reports the comparison between the solution obtained from the off-line optimal control problem used in the MOTP

Journal homepage: http://www.journals.elsevier.com/computers-and-chemical-engineering/
Original file available at: http://dx.doi.org/10.1016/j.compchemeng.2013.10.003

Postprint version of paper published in Computers & Chemical Engineering, 2014, Volume 61 Pages38–50.
The content is identical to the published paper, but without the final typesetting by the publisher.

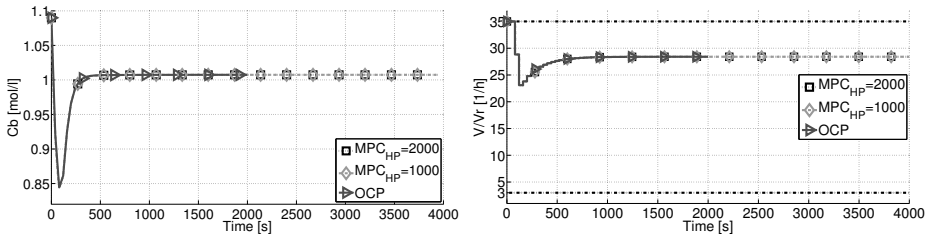

Figure 8: The two graphs show that no differences are present in the solutions obtained off-line and the on-line solution when halving the prediction horizon and under the assumption that no disturbance or model mismatch is present on the model

and two NMPC controllers with different lengths of the prediction horizon. In particular, the second controller has half of the length of the prediction horizon of the first one. Hence, the second controller has a prediction horizon and a control horizon of 1000 s. To enable a fair comparison the length of one piecewise constant control element remains unaltered, i.e., 40 s. Hence, the number of control elements in this second NMPC controller is now only 25 instead of 50 in the first one. Finally, also for the off-line optimal control problem the same length for a piecewise constant control element, i.e., 40 s is used, the end time is set to be 2000 s and the control discretisation is 50.

The off-line optimal control problem is solved for a time interval of 2000 s. Both NMPC controllers and the off-line optimal control problem used the same set of weights used for Scenario A. Under the assumption that no disturbance is present and that the mathematical model perfectly represents the real system, no difference is appreciable between the off-line solution and the on-line solutions with different lengths of prediction horizon. Hence, it can be argued that the optimal control problem solved in the MOTP and the on-line problem solved in the NMPC are defined to deliver identical solutions.

5.2.2. Influence of disturbances

It is important to state once again that the two objectives (i.e., Equations (34) and (35) are in conflict with each other. Hence, the behaviour of the plant will change according to the weight matrix used to build the global objective function (36). The proposed procedure allows for a clear understanding of the underlaying trade-offs between the single objective functions and can clearly indicate to the practitioner which weight matrix will be more

Journal homepage: http://www.journals.elsevier.com/computers-and-chemical-engineering/
Original file available at: http://dx.doi.org/10.1016/j.compchemeng.2013.10.003

adequately representing his/her preferences.

This section will investigate the effect of disturbances on the proposed procedure when different weight matrices are used to build the objective function used for the NMPC. The proposed problem is exactly the same presented in Section 5.1. The only difference is the presence of a random disturbance on the inlet flow concentration C_{a0}. Moreover, the results reported as Scenario B in Section 5.1 are adopted here as references. Hence, it is assumed that the practitioner responsible for the plant opted for a more careful control policy on the concentration of product B.

Figure 9 and Figure 10 report the response of the system when subjected to the disturbance in comparison with the selected reference trajectory. In particular, the left graph of Figure 9 clearly shows a significant difference in the response of the plant. Additionally, Table 4 reports the integral of the absolute value of the difference between the curves depicted in the left graph of Figure 9. It can be seen that the deviation from the reference trajectory obtained with the weight matrix of arbitrary weights, is around four times bigger then the deviation obtained with the weight matrix (called Dis: Scenario B) selected from the proposed procedure.

The main point here is that the set of weights obtained from the proposed tuning procedure allows for a more effective rejection of the disturbance on the interesting variable for the DM. In other words, here the focus should not be on the better performance achieved with one particular weight matrix or another but rather on the fact that once a weight matrix from the proposed tuning procedure is chosen this enables to preserve the DM's preferences even when the system is subjected to disturbances.

In fact, the results obtained with the set of arbitrary weights do not represent the intention of the DM who chose them. The intention was clearly to consider the concentration of product B and C equally important. In fact as it can be seen from Figure 9 and Figure 10 the trends obtained with the weight matrix of arbitrary weights reject the disturbance quite efficiently for the concentration of C and on the contrary allow for a significant fluctuation on the concentration of B. This is instead clearly avoided by the weight matrix selected from the proposed procedure which reduces the effect of the disturbance on the concentration of B while allowing for more fluctuation on

Postprint version of paper published in Computers & Chemical Engineering, 2014, Volume 61 Pages38–50.
The content is identical to the published paper, but without the final typesetting by the publisher.

Integrated Absolute Difference	
Concentration of B	
Ref - SB	10.27
Ref - AW	39.92

Table 4: Difference between trends followed by the state variables in the left graph in Figure 9. The reported numbers represent the integral of the absolute values of the difference of the two curves subjected to the disturbance with the reference.

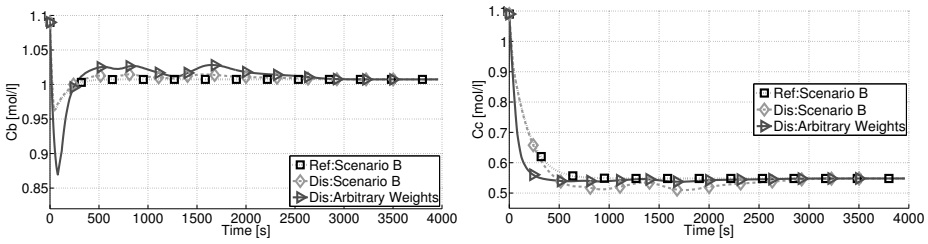

Figure 9: The two graphs reported here represent the behaviour of the plant when subjected to a random disturbance on the inlet flow concentration C_{a0}. The weight matrix used in this problem corresponds to the one identified by $\diamond$ in Figure 5. The left graph shows the trend followed by the concentration of product B, while the right one shows the trend for the concentration of by-product C.

the concentration of C.

In conclusion, the proposed tuning procedure is able to preserve the preference of the DM even when the system is subject to a disturbance. Additionally, the proposed tuning procedure appears particularly appealing for application in situations where disturbance rejection on specific variables is crucial, e.g., pressure control in vacuum or high pressurised equipment or temperature control when runaways can occur. Moreover, the NMPC controller adopted in this study also appears to be robust against significant disturbances.

5.2.3. Influence of model mismatch

Finally, the proposed procedure was tested under the assumption of a mismatch between the plant and the mathematical model used in the NMPC

Journal homepage: http://www.journals.elsevier.com/computers-and-chemical-engineering/
Original file available at: http://dx.doi.org/10.1016/j.compchemeng.2013.10.003

Postprint version of paper published in Computers & Chemical Engineering, 2014, Volume 61 Pages38–50.
The content is identical to the published paper, but without the final typesetting by the publisher.

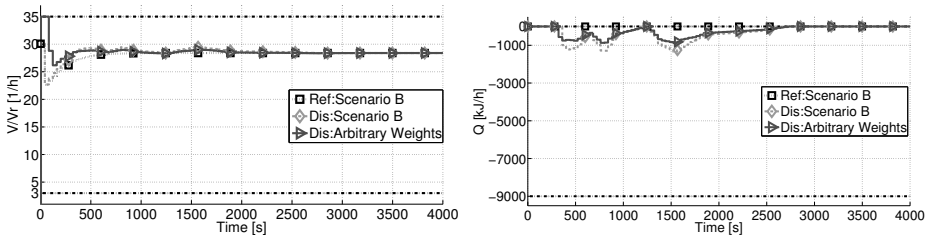

Figure 10: The two graphs reported here represent the behaviour of the plant when subjected to a random disturbance on the inlet flow concentration C_{a0}. The weight matrix used in this problem corresponds to the one identified by $\diamond$ in Figure 5. The left graph displays the control action for the inlet flow, while the right one illustrates the action for the duty in the jacket.

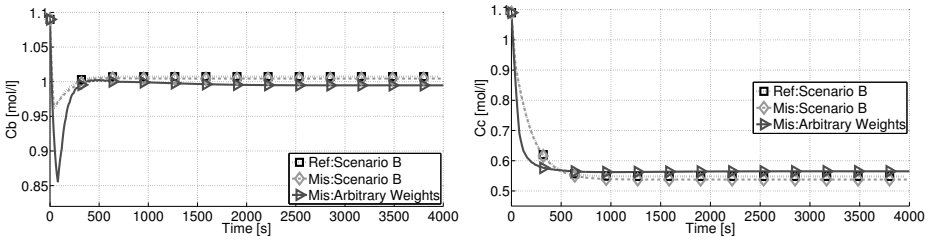

Figure 11: The two graphs reported here represent the behaviour of the plant when subjected to a model mismatch on reaction rate k_3. The weight matrix used in this problem corresponds to the ones used in Scenario B in Section 5.1. The left graph shows the trend followed by the concentration of product B, while the right one shows the trend for the concentration of waste product C.

controller. It is assumed that the reaction rate k_3 in Equation (26) is an order of magnitude bigger in the model used in the controller in respect to the reaction rate used in the model to simulate the reactor.

The two couples of graphs reported in Figure 11 and Figure 12 illustrate the results obtained with the model mismatch assumption. Once again it is possible to appreciate the different behaviours of the plant according to the weight matrix used to build the objective function. In particular, with reference to the left graph in Figure 11, it is interesting to notice how the solution obtained with the weight matrix $\diamond$ just exhibits a minimal off-set from the curve chosen as reference. On the other hand, the solution obtained with the arbitrary weight matrix shows a clear tendency to diverge from the

Journal homepage: http://www.journals.elsevier.com/computers-and-chemical-engineering/
Original file available at: http://dx.doi.org/10.1016/j.compchemeng.2013.10.003

Postprint version of paper published in Computers & Chemical Engineering, 2014, Volume 61 Pages38–50.
The content is identical to the published paper, but without the final typesetting by the publisher.

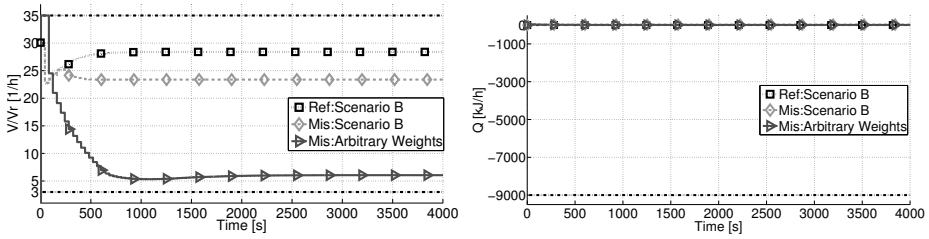

Figure 12: The two graphs reported here represent the behaviour of the plant when subjected a to a model mismatch on reaction rate k_3. The weight matrix used in this problem corresponds to the ones used in Scenario B in Section 5.1. The left graph displays the control action for the inlet flow, while the right one illustrates the action for the duty in the jacket.

Integrated Absolute Difference	
Concentration of B	
Ref - SB	10.85
Ref - AW	51.94

Table 5: Difference between trends followed by the state variables in the left graph in Figure 11. The reported numbers represent the integral of the absolute values of the difference of the two curves subjected to the model mismatch with the reference.

new given set-point.

As in the above section Table 5 reports the difference between the integral of the reference curve and the integral of the two curves obtained with the model mismatch. In this case, the deviation from the reference trajectory obtained by the implementation of the arbitrary weight matrix is five times bigger than the one obtained with the weight matrix $\diamond$. Additionally, the left graph of Figure 12 clearly indicates the significant difference in the control actions adopted by the NMPC according to the used weight matrix. In conclusion, even if the effects resulting from a model mismatch are less straightforward to analyse, due to the nonlinear relations involved, the weight matrix selected via the proposed procedure appears to preserve the preferences expressed by the DM.

Journal homepage: http://www.journals.elsevier.com/computers-and-chemical-engineering/
Original file available at: http://dx.doi.org/10.1016/j.compchemeng.2013.10.003

Postprint version of paper published in Computers & Chemical Engineering, 2014, Volume 61 Pages38–50.
The content is identical to the published paper, but without the final typesetting by the publisher.

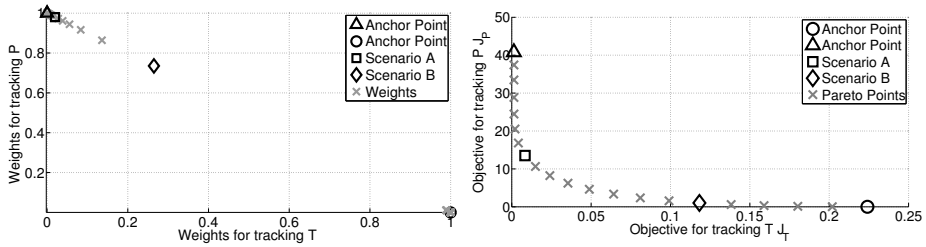

Figure 13: The graph on the right illustrates the set of weight matrices obtained via the MOTP with the two objectives reported in Equations (66) while the graph on the left reports the corresponding Pareto front. In particular the selected weight matrices successively implemented in the NMPC are identified by □ scenario A and ⋄ B .

5.3. Case Study II: Tennessee Eastman Reactor

In this section the results for the Tennessee Eastman reactor are presented. This case study is more complex and qualifies as a challenge for every nonlinear controller. The plant is subjected to a set point change, as described in [27, Jockenhövel et al., 2003], of 60 kPa from 2820 to 2760 kPa. No disturbance or model mismatch is considered for this application. However, based on results from previous section the procedure can deal with disturbances and (limited) model mismatches. As in the previous case change in operating condition is passed to the MOTP step which will provide the DM with the set of optimal control policies from which he/she can pick one. For this case study it is necessary to have a regularisation term in the objective function. Therefore the regularisation term was directly introduced in each of the two objectives as shown in Equation (66).

The value of the weight for the regularisation term was fixed at $R_{TE} = 0.01$. When formulating the NMPC objective function the two equations above summed, hence, the division of R_{TE} by two. Therefore, the MOTP has the task to return a set of weight matrices with two diagonal elements, w_1 and w_2.The optimal set of weight matrices obtained, carefully rescaled to take into consideration the regularisation term introduced, is reported in the right graph in Figure 13 while the left graph illustrates the corresponding Pareto set.

It can be seen that the weights in the left graph of Figure 13 appear to be quite clustered towards the pressure objective function. This clearly

Journal homepage: http://www.journals.elsevier.com/computers-and-chemical-engineering/
Original file available at: http://dx.doi.org/10.1016/j.compchemeng.2013.10.003

Postprint version of paper published in Computers & Chemical Engineering, 2014, Volume 61 Pages38–50.
The content is identical to the published paper, but without the final typesetting by the publisher.

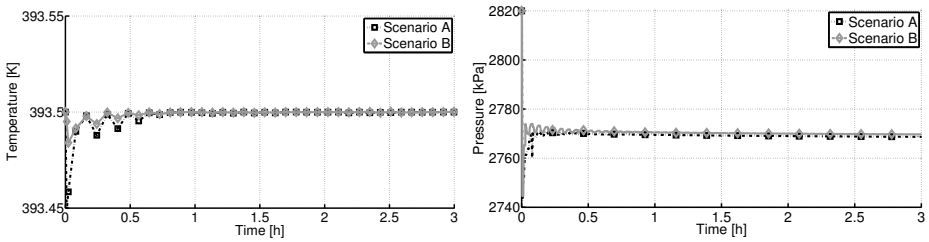

Figure 14: The two graphs reported here represent the behaviour of the plant when subjected to the different weight matrices identified by the two scenario A and B. The left graph depicts the trend followed by the manipulated flow of coolant in the reactor jacket, while the right one reproduces the trend for inlet flow of reactant E.

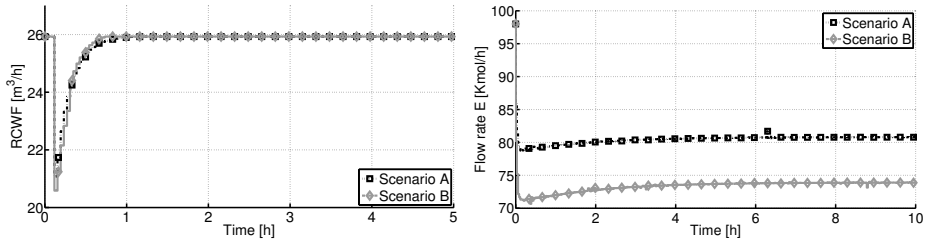

Figure 15: The two graphs reported here represent the behaviour of the plant when subjected to the different weight matrices identified by the two scenario A and B. The left graph illustrates the trend followed by the reactor pressure P, while the right one presents the trend for the reactor temperature.

indicates the importance of adequately controlling the pressure in this application. Two main aspects contributed to this result: *(i)* the pressure is the variable subjected to the step change and *(ii)* the double phase nature of the reactor itself.

At this point the decision maker can select which control policy to apply to move the system to the new operating point. As in the previous case two operating policies are selected for illustrative purposes, i.e., $\square$ for Scenario A (better tracking for P) and $\diamond$ for Scenario B (better tracking for T). Introducing the two weight matrices in the NMPC controller and performing the described step change of 60 kPa causes the system to behave as reported in Figures 14, 15 and 16.

Journal homepage: http://www.journals.elsevier.com/computers-and-chemical-engineering/
Original file available at: http://dx.doi.org/10.1016/j.compchemeng.2013.10.003

Postprint version of paper published in Computers & Chemical Engineering, 2014, Volume 61 Pages38–50.
The content is identical to the published paper, but without the final typesetting by the publisher.

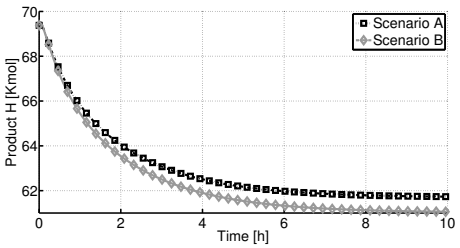

Figure 16: The graph reported here represents the behaviour of the plant when subjected to the different weight matrices identified by the two scenario A and B. In particular the amount of one for the two product H in the reactor is reported.

It has to be mentioned that the reported results are in accordance with the ones reported in [27, Jockenhövel et al., 2003]. However, it can be seen from the reported graphs that there is indeed a noticeable difference in the response of the plant, according to adopted weight matrix, i.e., control policy. From a practical point of view it can be argued that the major advantage of applying the proposed method for the selection of weights lies in the numerical quantification of the relative importance of the objectives. Additionally, it also highlight how it is unnecessary to use extreme numbers as weights to steer the control policy in the wanted direction. In fact it is sufficient to stick to a convex combination of weights to have a full range of operating conditions.

6. Conclusions

This work underlines the difficulties in performing the non-trivial task to tune an NMPC application. The mathematical reasons why such a selection of weights is not easy are presented. A systematic procedure based on advanced multi-objective optimisation methods is proposed and successfully applied to two different case studies. Additionally, the proposed procedure appears to be robust in the presence of disturbances of different nature, different NMPC settings and model mismatch. Moreover the weight matrices, chosen via the described procedure result from an optimal solution, thus ensuring the implementation of the desired control actions. Finally, when applied to the Van de Vusse reactor the Tennessee Eastman plant the procedures deliver satisfactory results. In particular, the procedure clearly identifies the relative importance of the single objective composing the global

Journal homepage: http://www.journals.elsevier.com/computers-and-chemical-engineering/
Original file available at: http://dx.doi.org/10.1016/j.compchemeng.2013.10.003

objective function and present the DM with a well defined set of possible control policies from which he/she can easily pick the preferred one. Hence, the proposed tuning procedure avoid the inefficient trial and error usually adopted to find a suitable weight matrix. For future work, a possible extention to Economic Model Predictive Control appears challenging to the authors. Furthermore, these results look promising as a step to rethink NMPC under a direct multi-objective approach.

7. Acknowledgements

Mattia Vallerio has a Ph.D. grant of the Agency for Innovation through Science and Technology in Flanders (IWT). Jan Van Impe holds the chair Safety Engineering sponsored by the Belgian Chemistry and Life Sciences Federation essenscia. The research was supported by KUL, OT/10/035, PFV/10/002 (OPTEC), IOF-SCORES4CHEM, the Flemish Government via FWO-projects: FWO-1518913N and FWO-G.0930.13 via IWT-projects, the Belgian Federal Science Policy Office: IAP VII/19 (DYSCO).

References

[1] J. Rawlings, Tutorial overview of model predictive control, IEEE Control Systems 20 (2000) 38–52.

[2] J. S. Qin, A. Badgwell, A survey of industrial model predictive control technology, Control Engineering Practice 11 (2003) 733–764.

[3] M. Diehl, H. Bock, J. Schlöder, R. Findeisen, Z. Nagy, F. Allgöwer, Real-time optimization and nonlinear model predictive control of processes governed by differential-algebraic equations, Journal of Process Control 12 (2002) 577–585.

[4] F. Manenti, Considerations on nonlinear model predictive control techniques, Computers and Chemical Engineering 35 (2011) 2491–2509.

[5] F. Allgower, T. A. Badgwell, J. S. Qin, J. B. Rawlings, S. J. Wright, Nonlinear predictive control and moving horizon estimation and introductory overview, in: Advances in Control, Highlights of ECC'99, pp. 391–449.

[6] M. Morari, J. H. Lee, Model predictive control: Past, present and future., Computers and Chemical Engineering 23 (1999) 667–682.

[7] L. Würth, R. Hannemann, W. Marquardt, Neighboring-extremal updates for nonlinear model-predictive control and dynamic real-time optimization, Journal of Process Control 19 (2009) 1277–1288.

[8] K. Miettinen, Nonlinear multiobjective optimization, Kluwer Academic Publishers, Boston, 1999.

[9] J. L. Garriga, M. Soroush, Model predictive control tuning methods: a review, Industrial & Engineering Chemistry Research 49 (2010) 3505–3515.

[10] W. Wojszniz, A. Mehta, P. Wojszniz, D. Thiele, T. Blevins, Multiobjective optimization for model predictive control, ISA transactions 46 (2007) 351–361.

[11] J. H. van der Lee, W. Svrcek, B. Young, A tuning algorithm for model predictive controllers based on genetic algorithms and fuzzy decision making, ISA transactions 47 (2008) 53–59.

[12] A. Bemporad, D. Muñoz de la Peña, Multiobjective model predictive control, Automatica 45 (2009) 2823–2830.

[13] V. Zavala, A. Flores-Tlacuahuac, Stability of multi objective predictive control: A utopia-tracking approach, Automatica 48 (2012) 2627–2632.

[14] A. Flores-Tlacuahuac, P. Morales, M. Rivera-Toledo, Multiobjective Non linear Model Predictive Control of a Class of Chemical Reactors, Industrial & Engineering Chemistry Research 51 (2012) 5891–5899.

[15] I. Das, J. Dennis, A closer look at drawbacks of minimizing weighted sums of objectives for Pareto set generation in multicriteria optimization problems, Structural Optimization 14 (1997) 63–69.

[16] I. Das, J. Dennis, Normal-Boundary Intersection: A new method for generating the Pareto surface in nonlinear multicriteria optimization problems, SIAM Journal on Optimization 8 (1998) 631–657.

Journal homepage: http://www.journals.elsevier.com/computers-and-chemical-engineering/
Original file available at: http://dx.doi.org/10.1016/j.compchemeng.2013.10.003

[17] A. Messac, A. Ismail-Yahaya, C. Mattson, The normalized normal constraint method for generating the Pareto frontier, Structural and Multidisciplinary Optimization 25 (2003) 86–98.

[18] J. Sanchis, M. Martinez, X. Blasco, J. Salcedo, A new perspective on multiobjective optimization by enhanced normalized normal constraint method, Structural and Multidisciplinary Optimization 36 (2008) 537–546.

[19] F. Logist, J. Van Impe, Novel insights for multi-objective optimisation in engineering using normal boundary intersection and (enhanced) normalised normal constraint, Structural and Multidisciplinary Optimization 45 (2012) 417–431.

[20] F. Manenti, S. Cieri, M. Restelli, N. M. N. Lima, L. Z. Linan, G. Bozzano, Online feasibility and effectiveness of a spatio-temporal nonlinear model predictive control. the case of methanol synthesis reactor, in: I. D. L. Bogle, M. Fairweather (Eds.), 22nd European Symposium on Computer Aided Process Engineering, volume 30 of *Computer Aided Chemical Engineering*, Elsevier, 2012, pp. 867 – 871.

[21] S. Dubljevic, P. D. Christofides, Predictive control of parabolic {PDEs} with boundary control actuation, Chemical Engineering Science 61 (2006) 6239 – 6248.

[22] B. Houska, H. Ferreau, M. Diehl, ACADO Toolkit - an open-source framework for automatic control and dynamic optimization, Optimal Control Applications and Methods 32 (2011) 298312.

[23] A. Messac, C. Mattson, Normal constraint method with guarantee of even representation of complete Pareto frontier, AIAA Journal 42 (2004) 2101–2111.

[24] F. Logist, M. Vallerio, B. Houska, M. Diehl, J. Van Impe, Multi-objective optimal control of chemical processes using ACADO toolkit, Computers and Chemical Engineering 37 (2012) 191–199.

[25] J. Bonilla Alarcon, M. Diehl, F. Logist, B. De Moor, J. Van Impe, A convexity-based homotopy method for nonlinear optimization in model predictive control, Optimal Control Applications & Methods 31 (2010) 393–414.

Journal homepage: http://www.journals.elsevier.com/computers-and-chemical-engineering/
Original file available at: http://dx.doi.org/10.1016/j.compchemeng.2013.10.003

[26] J. Downs, E. Vogel, A plant wide industrial process control problem, Computers and Chemical Engineering 17 (1993) 245–255.

[27] T. Jockenhövel, L. Biegler, A. Wächter, Dynamic optimization of the Tennessee Eastman process using the OptControlCentre, Computers and Chemical Engineering 27 (2003) 1513–1531.